Size and Temperature Dependence of Surface Plasmon Absorption of Gold Nanoparticles Induced by Tris(2,2′-bipyridine)ruthenium(II)

Xiao-Hong Nancy Xu,* Shuang Huang, William Brownlow, Khalid Salaita, and Robert B. Jeffers

Department of Chemistry and Biochemistry, Old Dominion University, Norfolk, Virginia 23529

Received: April 30, 2004; In Final Form: June 15, 2004

It is well known that surface plasmon absorption (color) of Au nanoparticles highly depends on its size, shape, and surrounding surface environment, providing a great opportunity for the development of Au nanoparticles as a probe for chemical and biochemical sensing and as a building block for nano-optical devices. Currently, it remains incompletely understood how the surface properties of Au nanoparticles ultimately define its optical properties, hindering the progress of rational design of Au nanoparticles for biochemical sensing and assembly of nano-optical devices. $Ru(bpy)_3^{2+}$ possesses rich photochemical and electrochemical properties, offering a unique probe to study the surface environment of Au nanoparticles. In this study, we investigate the kinetics of surface plasmon absorption of Au nanoparticles (6.5, 19, 48, 97 nm) in the presence of $Ru(bpy)_3^{2+}$ at 24.0, 33.0, and 51.0 °C. We find that the color-change rate of Au nanoparticles is highly sensitive to the amount of $Ru(bpy)_3^{2+}$. In addition, the minimum (critical) concentration of $Ru(bpy)_3^{2+}$ needed to change the color of Au nanoparticles is highly dependent upon temperature and nanoparticle size. TEM images illustrate that the color-change mechanism of Au nanoparticles induced by $Ru(bpy)_3^{2+}$ highly depends on the size of nanoparticles. Control experiments using NaCl and $MgCl_2$ to replace $Ru(bpy)_3^{2+}$ show no color change, suggesting that the color change of Au nanoparticles induced by $Ru(bpy)_3^{2+}$ is not solely attributable to the salt effect. Other factors, such as adsorption of $Ru(bpy)_3^{2+}$ on the Au nanoparticle surface, may be involved. Moreover, in the presence of the critical concentration of $Ru(bpy)_3^{2+}$, as temperature increases from 24.0 °C to 51.0 °C, the color-change rate of 19 nm Au nanoparticles increases 8-fold, whereas the color-change rate of 48 nm Au nanoparticles decreases 3-fold, showing the temperature dependence of surface plasmon absorption of Au nanoparticles in the presence of surface adsorbates, $Ru(bpy)_3^{2+}$.

Introduction

Colloidal gold (Au) nanoparticles have superior stability, uniform surface, and high affinity for organic functional groups. In addition, colloidal Au nanoparticles show unique size- and shape-dependent optical, electronic, and catalytic properties.[1−7] These unique features provide the possibility of developing biocompatible Au nanoparticles for bioanalysis,[8−17] interfacing Au nanoparticles with living cells,[13−17] and building nanoparticle blocks for nano-optical devices.[18] Surface plasmon absorption of Au nanoparticles depends on its size, shape, and surrounding surface environments (e.g., surface adsorbates and inter-nanoparticle spacing).[5−8] Unlike the bulk plasmon, the surface plasmon of Au nanoparticles can be directly excited by propagating light waves (electromagnetic waves), leading to the absorption and scattering of selective wavelengths of lights. Therefore, one could then tune the color of the nanoparticles by carefully controlling the size, shape, and surface environment of the nanoparticles. However, despite extensive studies over decades,[1−25] it still remains a challenge to precisely control the optical properties of Au nanoparticles. Furthermore, it is not yet fully understood how the surface adsorbates of Au nanoparticles affect the optical, electronic, and catalytical properties of the nanoparticles.[18−41] For instance, do the optical properties of Au nanoparticles depend on its surface-adsorbed species?[18−37] What mechanisms are involved?[18−40] Are the optical properties of Au nanoparticles sensitive to temperature in the presence of surface adsorbates?[3,4,21,41] These are key questions to be addressed in order to rationally design Au nanoparticles for biochemical sensing[8,12,15−17,34] and assembly of nano-optical devices.[42−44]

$Ru(bpy)_3^{2+}$ has rich photochemistry, photophysics, and photoredox properties. It provides intense absorption bands at 285 nm ($\epsilon = 1.2 \times 10^5$ M^{-1} cm^{-1}) and 452 nm ($\epsilon = 1.5 \times 10^4$ M^{-1} cm^{-1}) and gives off intensive phosphorescence at 600 nm with a quantum yield of 0.042 at ambient temperature.[45] In addition, $Ru(bpy)_3^{2+}$ is an electrochemically active species with reduction and oxidation potential at 1.04 V and 1.18 V vs SCE, respectively. Moreover, $Ru(bpy)_3^{2+}$ produces electrochemiluminescence in the presence of co-reactors (e.g., tripropylamine (TPA)).[45−47] These unique characteristics make $Ru(bpy)_3^{2+}$ a powerful probe for a variety of applications including DNA sensing,[48] analysis of tumor markers, and study of protein−protein interactions.[49] Previous studies have demonstrated that $Ru(bpy)_3^{2+}$ directly adsorbed on the Au surface using the hydrophobic interaction of tris-bipyridine with the surface Au atoms.[50]

In this study, we select $Ru(bpy)_3^{2+}$ as a probe to study the dependence of optical properties of Au nanoparticles upon its surface environment because the unique optical and electrochemical properties of $Ru(bpy)_3^{2+}$ offer the great opportunity to probe the surface properties of Au nanoparticles using an array of ultrasensitive detection means. Furthermore, the study of the photochemical and photocatalytic properties of $Ru(bpy)_3^{2+}$

* To whom correspondence should be addressed. E-mail: xhxu@odu.edu; www.odu.edu/sci/xu/xu.htm. Tel/fax: (757) 683-5698.

10.1021/jp048124b CCC: $27.50
Published on Web 09/16/2004

adsorbed on the surface of Au nanoparticles is also an interesting and important topic.

In previous studies, Ru(II) tris(2,2′-bipyrridine)cyclobis-(paraquat-*p*-phenylene) catenane was used as a photosensitizer to cross-link Au nanoparticle arrays for photoelectrochemical and electrochemical sensing.[42−44] The emission of $Ru(bpy)_3^{2+}$ quenched by Au nanoparticles has also been reported.[51] Unlike these previously reported studies, we will describe the dependence of surface plasmon absorption (color) upon the size of the nanoparticles, the amount of surface-adsorbed $Ru(bpy)_3^{2+}$, and temperature. To the best of our knowledge, surface plasmon absorption of Au nanoparticles as a function of nanoparticle size and temperature in the presence of $Ru(bpy)_3^{2+}$ has not yet been reported. This study provides new opportunities to probe surface and optical properties of Au nanoparticles, the coagulation rate of the nanoparticles,[21] the chemical interface damping model,[52,53] and photochemistry and photocatalytical properties of $Ru(bpy)_3^{2+}$ on Au nanoparticle surfaces and to develop Au nanoparticles for ultrasensitive sensing and nano-optics.

Experimental Section

Chemicals and Materials. $HAuCl_4 \cdot 2H_2O$, sodium citrate dihydrate, tannic acid, and $Ru(bpy)_3Cl_2 \cdot H_2O$ were purchased from Aldrich and used as received without further purification. Ultrapure water (Nanopore, 18 MΩ, sterilized) is used to prepare all solutions and to synthesize Au nanoparticles. The stock solution of 45.5 μM $Ru(bpy)_3^{2+}$ is prepared using ultrapure water and stored in a light-protected container at 4 °C.

Synthesis and Characterization of Au Nanoparticles. The Au nanoparticles with a diameter of 6.5, 19, 48, and 97 nm are prepared using the synthesis procedures as described previously.[13,15,16,54] Glassware is cleaned with aqua regia (3:1 of HCl to HNO_3), rinsed with ultrapure water, and then dried prior to use. The 6.5 nm Au nanoparticles are prepared as follows: (i) a mixture of freshly prepared tri-sodium citrate (10 mL, 1%) and tannic acid (2.25 mL, 1%) is rapidly added into stirring and refluxing $HAuCl_4$ (0.01%, 500 mL), leading to a color change of solution from yellow to violet within seconds. (ii) The solution is refluxed for an additional 5 min, cooled to room temperature, and subsequently filtered using a 0.22 μm filter. The Au nanoparticles of 19, 48, and 97 nm are prepared by adding 50 mL of 38.8 mM, 5 mL of 1%, and 2.1 mL of 1% freshly prepared sodium citrate into stirring and refluxing $HAuCl_4$ (0.01%, 500 mL), respectively. The solutions are refluxed for an additional 15 min, cooled to room temperature, and subsequently filtered using a 0.22 μm filter.

These Au nanoparticles are characterized using UV−vis spectroscopy (U 2010, Hitochi and Cary-3G, Varian) and transmission electron microscopy (TEM) (JEOL 100CX). Au nanoparticles are prepared on 100 mesh Formvar-coated copper grids (Electron Microscopy Sciences) for TEM imaging.

The concentrations of the Au nanoparticles are calculated as follows. The weight of Au (W_{Au}) produced from the complete reduction of $HAuCl_4$ is calculated by multiplying the moles of added $HAuCl_4$ (weight of added $HAuCl_4 \cdot 2H_2O$ divided by molecular weight (MW) of $HAuCl_4 \cdot 2H_2O$) with the atomic weight of Au (196.97 g/mol). The volume of generated Au (V_{Au}) is calculated by dividing the weight of produced Au (W_{Au}) by the density of Au ($d = 19.32$ g/cm^3), as $V_{Au} = W_{Au}/d$. The number of Au nanoparticles (diameter (D) = 6.5, 19, 48, 97 nm) is computed by dividing the volume of generated Au (V_{Au}) by the volume of an individual Au nanoparticle ($\pi D^3/6$). The moles of Au nanoparticles are then determined by dividing the number of Au nanoparticles by Avogadro's constant (6.02×10^{23}). Finally, the molar concentrations of Au nanoparticles are calculated by dividing the moles of Au nanoparticles by the solution volume. Using this approach, the concentration of 6.5, 19, 48, and 97 nm Au nanoparticles is determined as 29.9 nM, 4.3 nM, 74 pM, and 8.2 pM, respectively. The 6.5, 19, and 48 nm Au nanoparticle solutions are diluted 10 times and the 97 nm Au nanoparticle solution is diluted 3 times using ultrapure water prior to its titration with $Ru(bpy)_3^{2+}$.

Titration of Au Nanoparticle Solution with $Ru(bpy)_3^{2+}$. The diluted Au nanoparticle solution of 2500 μL is used for all titration experiments. In these experiments, the Au nanoparticle solution is mixed with a variety of microliters of $Ru(bpy)_3^{2+}$ solution (45.5 μM) and ultrapure water to prepare a final solution of 3500 μL. Thus, the final concentration of 6.5, 19, 48, and 97 nm Au nanoparticles is 2.13 nM, 0.36 nM, 6 pM, and 2 pM, respectively.

Ultrapure H_2O and 2500 μL of Au nanoparticle solution are first added into a clean quartz cuvette (optical path 10 mm). A timer is started simultaneously as $Ru(bpy)_3^{2+}$ solution is mixed with the Au nanoparticle solution in the cuvette. The cuvette with a tightened cap is quickly reversed several times to well mix the solution and then is inserted into the cuvette holder in the UV−vis spectrometer. The absorbance spectra of the mixture are recorded over 2 h by repeatedly scanning wavelengths from 200 to 800 nm (Figures 1A−4A). Different quantities of $Ru(bpy)_3^{2+}$ are used to titrate the Au nanoparticle solution to determine the minimal (critical) concentration of $Ru(bpy)_3^{2+}$ that is needed to change the color of Au nanoparticle solution. Plots of baseline-subtracted peak absorbance versus time at the corresponding $Ru(bpy)_3^{2+}$ concentration are used to determine the dependence of color-change kinetics upon $Ru(bpy)_3^{2+}$ concentration (Figures 1B−4B). After the Au nanoparticle solutions have been measured using UV−vis spectroscopy over 2 h (Figures 1A−4A), TEM samples of the Au nanoparticle solutions in the absence and presence of $Ru(bpy)_3^{2+}$ are prepared on 100 mesh Formvar-coated copper grids and imaged using TEM (Figures 1−4, C, D).

Temperature Dependence Experiment. A circulating water bath of a UV/vis spectrometer (Cray 3G Varian) is used to maintain solution temperature in the cuvettes at 24.0, 33.0, and 51.0 °C, respectively. To maintain a homogeneous mixture and temperature, a tiny stirring bar is used to mix the solution in the cuvette during the experiments. Using the same approach as described above in the titration experiments, the minimal (critical) concentration of $Ru(bpy)_3^{2+}$ for the color change of Au nanoparticles at 33.0 °C is determined. Plots of baseline-subtracted peak absorbance versus time in the presence of the critical concentration of $Ru(bpy)_3^{2+}$ at 24.0, 33.0, and 51.0 °C are used to study the temperature dependence of the color-change rate of the Au nanoparticle solution (Figure 5). Two sizes of Au nanoparticles, 19 and 48 nm, are selected to investigate whether the temperature dependence of the color-change kinetics is associated with the size of nanoparticles.

Results and Discussion

Synthesis and Characterization of Au Nanoparticles. The Au nanoparticles are synthesized as described above and are characterized using UV−vis spectroscopy and TEM (Figures 1−4), showing that the surface plasmon absorption of Au nanoparticles occurs at a peak absorbance wavelength (λ_{max}) of 519, 524, 531, and 545 nm for the sizes of nanoparticles of 6.5 ± 1.5, 18.6 ± 3.5, 48.1 ± 5.8, and 96.7 ± 15.4 nm, respectively. The peak wavelength indicates a red shift with a broader bandwidth as the size of nanoparticles increases,

demonstrating that the surface plasmon absorption of Au nanoparticles shows size dependence. As reported in the literature, the intense color of Au nanoparticles is attributable to collective oscillation of free conduction electrons.[5−7] These conduction electrons (surface plasmon) resonate with the incident photon frequency, leading to specific absorbance in a visible range.[5−7]

The extinction coefficient of 6.5, 19, 48, and 97 nm Au nanoparticles is about 3, 4, 5, and 6 orders of magnitude greater than that of $Ru(bpy)_3^{2+}$, respectively. Therefore, the absorbance of $Ru(bpy)_3^{2+}$ at 285 nm ($\epsilon = 1.2 \times 10^5$ M^{-1} cm^{-1}) and 452 nm ($\epsilon = 1.5 \times 10^4$ M^{-1} cm^{-1}) in Figures 1−4 appears not to interfere with the absorbance of Au nanoparticles at 524 nm.

Dependence of Color-Change Kinetics upon Nanoparticle Size and $Ru(bpy)_3^{2+}$ Concentration. The Au nanoparticles are surrounded by excess citrate anions, resulting in the negatively charged Au nanoparticle surface. The electrostatic repulsion among the nanoparticles prevents the Au nanoparticles from aggregation. The addition of $Ru(bpy)_3^{2+}$ into the Au nanoparticles may lead to the color change of Au nanoparticle solution because $Ru(bpy)_3^{2+}$ is a multicharged cation and could neutralize the negative charges on the Au nanoparticle surface and decrease the ξ potential on the Au nanoparticle surface. This salt effect may bring individual Au nanoparticles into very close contact and hence change the inter-nanoparticle spacing, leading to the inter-nanoparticle plasmon coupling and an additional absorption peak at a longer wavelength beyond 600 nm. Consequently, the color of the Au nanoparticle solution would be changed from pink to blue.

To study whether the color change of Au nanoparticles induced by $Ru(bpy)_3^{2+}$ depends on the size of nanoparticles, we select 6.5, 19, 48, and 97 nm Au nanoparticles to determine the minimum (critical) concentration of $Ru(bpy)_3^{2+}$ that is needed to change the color of Au nanoparticle solutions from pink to blue. The color-change kinetics of Au nanoparticle solutions in the presence of the critical concentration of $Ru(bpy)_3^{2+}$ are investigated to understand its dependence upon nanoparticle size. We have attempted to prepare the same concentration of different sizes of Au nanoparticles for their titration experiments with $Ru(bpy)_3^{2+}$. Unfortunately, it is impossible to perform the experiment using the same concentration of the different size Au nanoparticles because 0.36 nM of the 97 nm Au nanoparticles tend to be aggregated. In contrast, 2 pM of the 19 nm Au nanoparticles show invisible absorbance because the extinction coefficient of the 97 nm Au nanoparticle is about 2 orders of magnitude larger than that of the 19 nm Au nanoparticles. Therefore, 2.13 nM, 0.36 nM, 6 pM, and 2 pM of 6.5, 19, 48, and 97 nm Au nanoparticles are selected to maintain the total surface Au atoms in each Au nanoparticle solution nearly comparable at 7×10^{15}, 1×10^{16}, 1×10^{15}, and 2×10^{15}, respectively. The total number of surface Au atoms is calculated by dividing the surface area of all Au nanoparticles (πD^2 *NCV*) by the area of an individual Au atom (diameter of Au atom (d_{Au}) = 0.288 nm; area = d_{Au}^2) using a close-pack model, where *D*, *N*, *C*, and *V* refer to diameter of an individual Au nanoparticle (*D* = 6.5, 19, 48, and 97 nm), Avogadro's constant (6.02×10^{23}), molar concentration of Au nanoparticles, and volume of Au nanoparticle solution, respectively.

For the 6.5 nm Au nanoparticles, 2.13 nM Au nanoparticle solutions are titrated with $Ru(bpy)_3^{2+}$. The absorbance spectra of the Au nanoparticles incubated with 0.142 μM $Ru(bpy)_3^{2+}$ are recorded over 2 h at 5 min intervals. The spectra remain nearly constant (Figure 1A). The peak absorbance of the 6.5 nm Au nanoparticles at 519 nm in the absence and presence of $Ru(bpy)_3^{2+}$ (0−0.142 μM) remains unchanged, as shown in Figure 1B, indicating that the color of the Au nanoparticle solution remains unchanged over time. TEM images of the Au nanoparticles that have already been incubated with 0 and 0.142 μM $Ru(bpy)_3^{2+}$ for 2 h demonstrate that individual Au nanoparticles are well isolated, as illustrated in Figure 1C, D. This result suggests that 0.142 μM $Ru(bpy)_3^{2+}$ is unable to cause the aggregation of 2.13 nM of 6.5 nm Au nanoparticles. Increasing the titration concentration of $Ru(bpy)_3^{2+}$ up to 1.3 μM still leaves the peak absorbance (color) of the Au nanoparticle solution unchanged. The absorbance of 1.3 μM $Ru(bpy)_3^{2+}$ at 452 nm appears to interfere with the measurement of Au nanoparticle absorbance at 519 nm, which prevents the higher concentrations of $Ru(bpy)_3^{2+}$ from being used in the titration experiment.

To determine whether the salt effect (neutralization of surface charges of Au nanoparticles) can lead to the color change of the Au nanoparticles, 568 nM NaCl and $MgCl_2$ are used to incubate with 2.13 nM of 6.5 nm Au nanoparticles and the spectra of the Au nanoparticle solutions are recorded over 2 h. Plots of peak absorbance of the Au nanoparticles versus time indicate that the peak absorbance remains constant, showing neither 568 nM NaCl nor $MgCl_2$ can cause the color change of the 6.5 nm Au nanoparticle. TEM images of the Au nanoparticle solution containing 568 nM NaCl or $MgCl_2$ are the same as observed in Figure 1C, D, indicating that the Au nanoparticles are not aggregated in the presence of 568 nM NaCl or $MgCl_2$.

For the 19 nm Au nanoparticles, 0.36 nM Au nanoparticle solutions are titrated by $Ru(bpy)_3^{2+}$, indicating that a concentration of $Ru(bpy)_3^{2+}$ beyond 107 nM changes the color of Au nanoparticles from pink to blue. The absorbance spectra of the 0.36 nM Au nanoparticles incubated with 114 nM $Ru(bpy)_3^{2+}$ are recorded over 2 h, showing that the absorbance of Au nanoparticles at 524 nm decreases over time as a broader absorbance peak at a longer wavelength (650 nm) appears and increases with time (Figure 2A). In contrast, the peak absorbance of the 19 nm Au nanoparticles at 524 nm in the absence and presence of lower concentrations of $Ru(bpy)_3^{2+}$ (0−95 nM) remains unchanged, as shown in Figure 2B. Taken together, the results in Figure 2B show that the peak absorbance of 0.36 nM of 19 nm Au nanoparticles decreases with time in the presence of $Ru(bpy)_3^{2+}$ concentrations of 107, 112, 114, 119, and 131 nM, indicating that the minimum (critical) concentration of $Ru(bpy)_3^{2+}$, 107 nM, is needed to change the color of the Au nanoparticles at room temperature.

The results in Figure 2B also indicate that the rate of decreased absorbance (color change) of Au nanoparticles is highly sensitive to the presence of $Ru(bpy)_3^{2+}$ concentration. For example, the absorbance of Au nanoparticles in the presence of 95 nM $Ru(bpy)_3^{2+}$ remains constant. In contrast, the absorbance of the Au nanoparticles in the presence of 107 nM $Ru(bpy)_3^{2+}$ decreases with time gradually at a rate of 4.9×10^{-4} min^{-1} and reaches equilibrium at an absorbance of 0.1285. As $Ru(bpy)_3^{2+}$ concentration increases to 131 nM, the absorbance of Au nanoparticles decreases with time dramatically at the rate of 5.7×10^{-3} min^{-1} and reaches equilibrium at an absorbance of 0.056. The slopes of peak absorbance of Au nanoparticles versus time in the presence of 112 and 114 nM $Ru(bpy)_3^{2+}$ are clearly distinguished with a rate of 9.8×10^{-4} min^{-1} and 2.5×10^{-3} min^{-1}, respectively (Figure 2B), demonstrating that the color-change rate is highly sensitive to the quantity of $Ru(bpy)_3^{2+}$, and colorimetry of Au nanoparticles

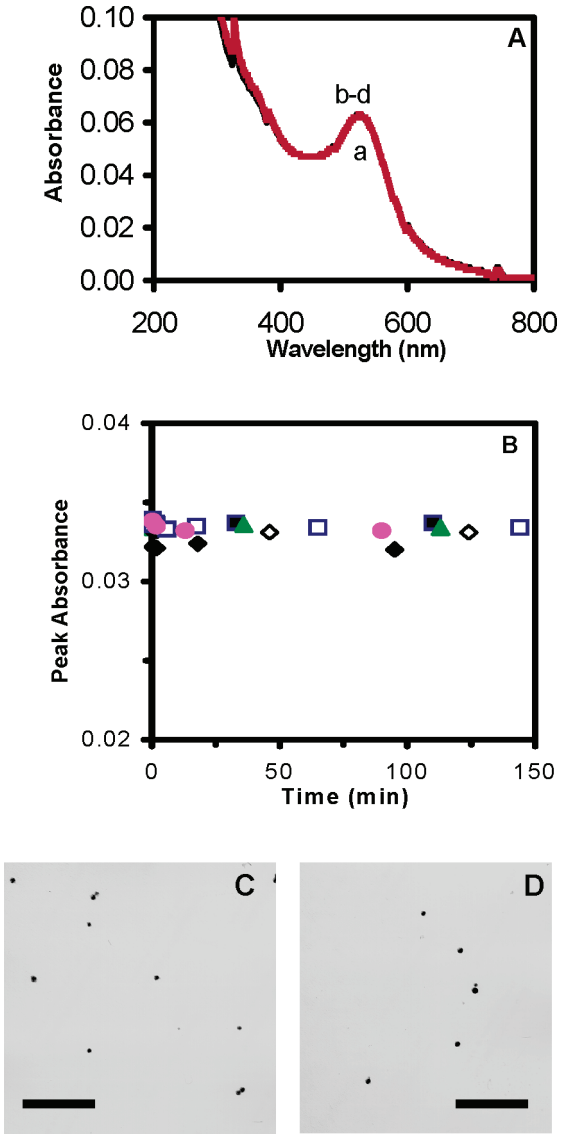

Figure 1. Representative UV−vis absorbance spectra of 2.13 nM Au nanoparticles (6.5 nm) in the absence and presence of $Ru(bpy)_3^{2+}$ at 24 °C. (A) Absorbance spectra are taken from the Au nanoparticle solutions incubated with 0−142 nM $Ru(bpy)_3^{2+}$ for (a) 0 to (b−d) 2 h. (B) Plots of baseline-subtracted peak absorbance at 519 nm versus time are constructed from the absorbance spectra of the Au nanoparticle solutions incubated with $Ru(bpy)_3^{2+}$ concentrations at (◆) 107 nM, (■) 114 nM, (▲) 119 nM, (◇) 131 nM, (□) 142 nM, and (●) 568 nM NaCl or $MgCl_2$. TEM images are acquired from 2.13 nM of the 6.5 nm Au nanoparticle solutions that have already been incubated with (C) 0 and (D) 142 nM $Ru(bpy)_3^{2+}$ for 2 h. The scale bar represents 94 nm.

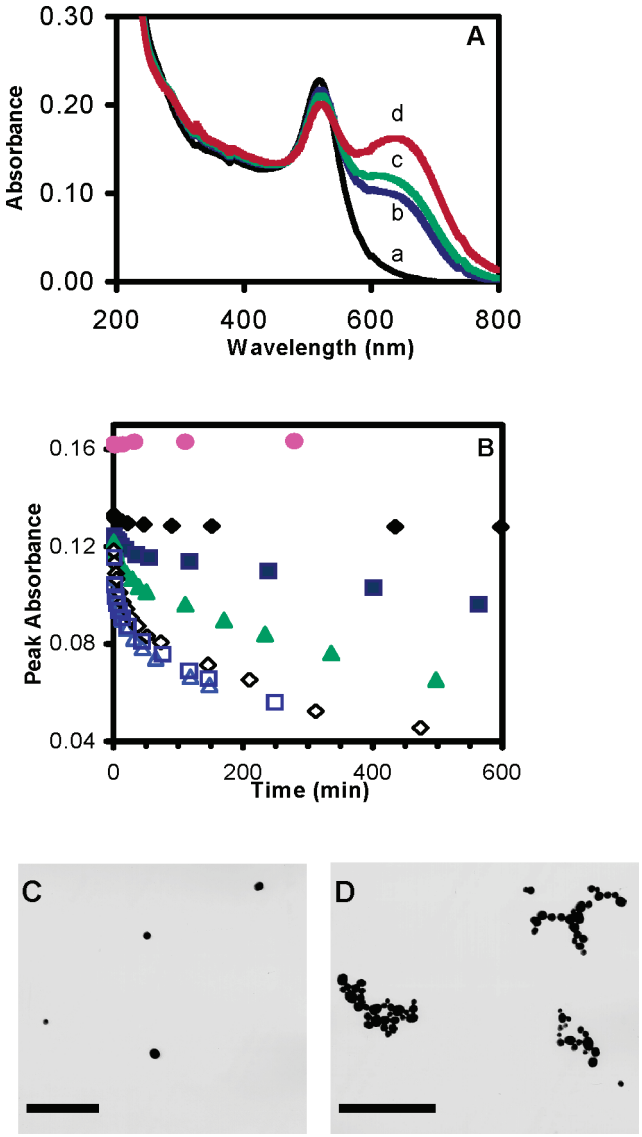

Figure 2. Representative UV−vis absorbance spectra of 0.36 nM Au nanoparticles (19 nm) in the absence and presence of $Ru(bpy)_3^{2+}$ at 24 °C. (A) Absorbance spectra are recorded from the Au nanoparticle solutions incubated with 114 nM $Ru(bpy)_3^{2+}$ at (a) 0 min (Au nanoparticles only), (b) 0.33 min, (c) 10.83 min, (d) 163 min. (B) Plots of the baseline-subtracted peak absorbance at 524 nm versus time are constructed from the absorbance spectra of Au nanoparticle solutions incubated with $Ru(bpy)_3^{2+}$ concentrations at (◆) 95 nM, (■) 107 nM, (▲) 112 nM, (◇) 114 nM, (□) 119 nM, (△) 131 nM, and (●) 524 nM NaCl or $MgCl_2$. TEM images are acquired from 0.360 nM of the 19 nm Au nanoparticle solutions that have already been incubated with (C) 0 and (D) 107−131 nM $Ru(bpy)_3^{2+}$ for 2 h. The scale bar represents 137 nm.

can be used to differentiate 7 pmol of $Ru(bpy)_3^{2+}$ [(114 − 112) nM = 2 nM in 3.5 mL solution; 2 nM × 3.5 mL = 7 pmol)] (Figure 2B).

TEM images acquired from the Au nanoparticle solutions that have already been incubated with 0 and 131 nM $Ru(bpy)_3^{2+}$ for 2 h show that the individual nanoparticles are well isolated in the absence of $Ru(bpy)_3^{2+}$ and become coagulated in the presence of 131 nM $Ru(bpy)_3^{2+}$, suggesting that the color change of Au nanoparticles is attributable to the aggregation of Au nanoparticles.

To determine whether the color change of Au nanoparticle solution induced by $Ru(bpy)_3^{2+}$ is solely contributed by the salt effect of $Ru(bpy)_3^{2+}$, the 0.360 nM of 19 nm Au nanoparticle solution is incubated with 524 nM NaCl or $MgCl_2$, a concentration that is 4-fold higher than the critical concentration of $Ru(bpy)_3^{2+}$. The spectra of the Au nanoparticle solution containing 524 nM NaCl or $MgCl_2$ are recorded over 2 h. Plots of baseline-subtracted peak absorbance of Au nanoparticles versus time show that the peak absorbance remains constant, indicating that neither 524 nM NaCl nor $MgCl_2$ changes the color of the Au nanoparticles (Figure 2B). TEM images of the 0.360 nM Au nanoparticle solutions incubated with 524 nM NaCl or $MgCl_2$ for 2 h are similar to those observed in Figure 2C, showing that the individual Au nanoparticles are well isolated. This experiment suggests that the color change of Au nanoparticle solution appears not to be solely attributable to the neutralization of negative charges on the Au nanoparticle surface by $Ru(bpy)_3^{2+}$ (salt effect). Other factors, such as the

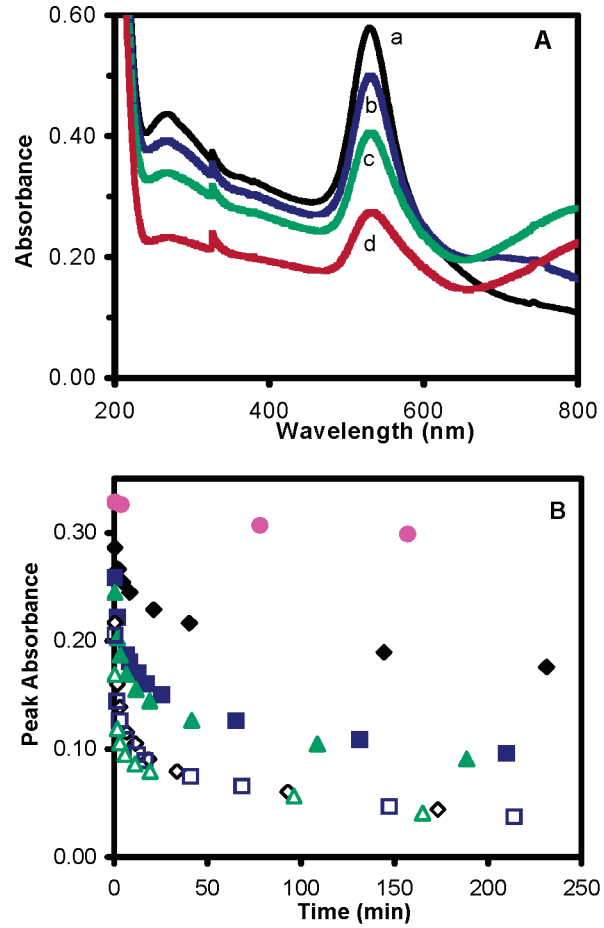

Figure 3. Representative UV−vis absorbance spectra of 6 pM Au nanoparticles (48 nm) in the absence and presence of $Ru(bpy)_3^{2+}$ at 24 °C. (A) Absorbance spectra are recorded from the Au nanoparticle solutions incubated with 83 nM $Ru(bpy)_3^{2+}$ at (a) 0 min, (b) 0.28 min, (c) 8.33 min, (d) 131.5 min. (B) Plots of baseline-subtracted peak absorbance at 524 nm versus time are constructed from the Au nanoparticle solution incubated with $Ru(bpy)_3^{2+}$ concentrations at (◆) 76 nM, (■) 83 nM, (▲) 95 nM, (◇) 107 nM, (□) 119 nM, (△) 142 nM, and (●) 570 nM NaCl or $MgCl_2$. TEM images are acquired from 6 pM of the 48 nm Au nanoparticle solutions that have already been incubated with (C) 0 and (D) 107 nM $Ru(bpy)_3^{2+}$ for 2 h. The scale bar represents 288 nm.

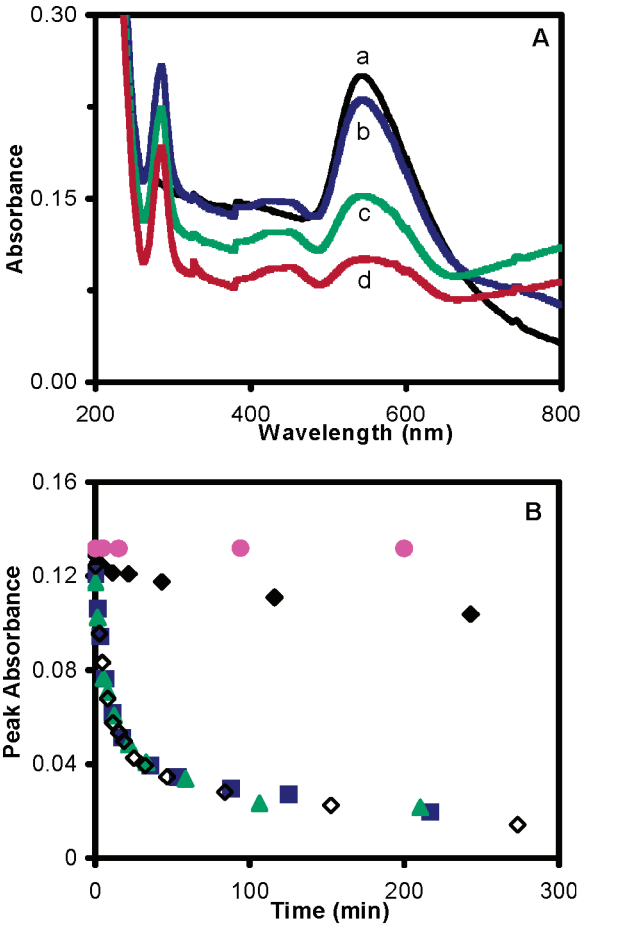

Figure 4. Representative UV−vis absorbance spectra of 2 pM Au nanoparticles (97 nm) in the absence and presence of $Ru(bpy)_3^{2+}$ at 24 °C. (A) Absorbance spectra are acquired from the Au nanoparticle solutions incubated with 1.22 μM $Ru(bpy)_3^{2+}$ at (a) 0 min, (b) 0.27 min, (c) 11.5 min, (d) 125 min. (B) Plots of baseline-subtracted peak absorbance at 524 nm versus time are constructed from the Au nanoparticle solutions incubated with $Ru(bpy)_3^{2+}$ concentration at (◆) 1.17 μM, (■) 1.22 μM, (▲) 1.27 μM, (◇) 1.30 μM, and (●) 5.20 μM NaCl or $MgCl_2$. TEM images are acquired from 2 pM of the 97 nm Au nanoparticle solutions that have already been incubated with (C) 0 and (D) 1.30 μM $Ru(bpy)_3^{2+}$ for 2 h. The scale bar represents 151 nm.

adsorption of $Ru(bpy)_3^{2+}$ on the surface of Au nanoparticles and possible reaction between $Ru(bpy)_3^{2+}$ and Au nanoparticles, may play a significant role in changing the color of the Au nanoparticle solution.

For the 48 nm Au nanoparticles, 6 pM Au nanoparticle solutions are titrated by $Ru(bpy)_3^{2+}$ (Figure 3). The spectra of the 48 nm Au nanoparticles in the presence of 83 nM $Ru(bpy)_3^{2+}$ show that the absorbance of the Au nanoparticles at 531 nm decreases with time as a broader absorbance peak beyond 800 nm appears and increases with time (Figure 3A). Plots of baseline-subtracted peak absorbance versus time in Figure 3B indicate that the critical concentration of $Ru(bpy)_3^{2+}$ at 83 nM is needed to change the color of 6 pM of the 48 nm Au nanoparticles from pink to blue. The rate of decreased absorbance (color change) of the Au nanoparticles at 531 nm is highly dependent upon the quantity of $Ru(bpy)_3^{2+}$ (Figure 3B). For instance, the peak absorbance of the 48 nm Au nanoparticle solution containing 76 nM $Ru(bpy)_3^{2+}$ decreases with time gradually at the rate of 7×10^{-3} min^{-1} and reaches equilibrium at an absorbance of 0.1757. In contrast, the absorbance of the 48 nm Au nanoparticles in the presence of 83 nM $Ru(bpy)_3^{2+}$ decreases with time dramatically at the rate of 1×10^{-2} min^{-1} and reaches equilibrium at an absorbance of 0.096. TEM images

of the 48 nm Au nanoparticle solutions in the absence and presence of $Ru(bpy)_3^{2+}$ (0, 107 nM) in Figure 3C, D indicate that the individual Au nanoparticles are well isolated in the absence of $Ru(bpy)_3^{2+}$ and become coagulated in the presence of 107 nM $Ru(bpy)_3^{2+}$, suggesting that the coagulation of Au nanoparticles is indeed involved in the color change of the Au nanoparticle solution. The control experiment is carried out by incubation of 6 pM of the 48 nm Au nanoparticles with 570 nM NaCl or $MgCl_2$ (4-fold higher than the critical concentration of $Ru(bpy)_3^{2+}$), showing no color change of the Au nanoparticle solution. TEM images of the 48 nm Au nanoparticle solutions incubated with 570 nM NaCl or $MgCl_2$ for 2 h are similar to those observed in the absence of $Ru(bpy)_3^{2+}$, indicating well-isolated individual Au nanoparticles (Figure 3C). As observed in the 19 nm Au nanoparticles, these TEM images demonstrate that the color change of the 48 nm Au nanoparticle solution by $Ru(bpy)_3^{2+}$ appears to be attributable not only to the salt effect but also to other factors.

Using the same approach, the color change of the 97 nm Au nanoparticles (2 pM) induced by $Ru(bpy)_3^{2+}$ is studied and shown in Figure 4. The spectra of the 97 nM Au nanoparticles in the presence of 1.22 μM $Ru(bpy)_3^{2+}$ in Figure 4A show that the peak absorbance of the 97 nm Au nanoparticles at 545 nm decreases with time as a broader peak at a long wavelength beyond 800 nm appears and increases with time. In this experiment, the higher concentration (1.22 μM) of $Ru(bpy)_3^{2+}$ is used. Therefore, the absorbance of $Ru(bpy)_3^{2+}$ at 281 and 452 nm is observed with the addition of $Ru(bpy)_3^{2+}$ (Figure 4A, b). The absorbance of the Au nanoparticle solution decreases with time, lowering the baseline of absorption spectra of Au nanoparticles. The peak absorbance of 1.22 μM $Ru(bpy)_3^{2+}$ at 281 and 452 nm actually remains almost constant because the decreased absorbance is attributable to the lower baseline of the spectra, suggesting that the quantity of $Ru(bpy)_3^{2+}$ remains almost unchanged over incubation time.

Note that the large Au nanoparticles (97 nm) create a slightly higher absorbance baseline than the small nanoparticles (Figures 1A−4A), because Rayleigh scattering of Au nanoparticles increases proportionally as the volume of nanoparticles increases. The large nanoparticles (97 nm) scatter light more effectively than the small nanoparticles, reducing the transmittance, which leads to the higher absorbance baseline. The peak absorbance of the Au nanoparticles in Figures 1B−4B and 5 has been corrected by its baseline absorbance. The change of baseline-subtracted peak absorbance is used to measure the color-change rate of the Au nanoparticles.

As observed in the 19 and 48 nm Au nanoparticle solutions, plots of baseline-subtracted peak absorbance of 2 pM of 97 nm Au nanoparticle solutions containing 1.17, 1.22, 1.27, and 1.30 μM $Ru(bpy)_3^{2+}$ versus time in Figure 4B indicate that the rate of decreased absorbance (color change) of Au nanoparticles is highly dependent upon the amount of $Ru(bpy)_3^{2+}$. In 1.17 μM $Ru(bpy)_3^{2+}$, the peak absorbance of the 97 nm Au nanoparticle solution at 545 nm decreases with time slightly at a rate of 1×10^{-3} min^{-1} and reaches equilibrium at an absorbance of 0.104. In contrast, the absorbance of Au nanoparticles decreases dramatically in the presence of $Ru(bpy)_3^{2+}$ concentration beyond 1.22 μM at a rate of 7×10^{-3} min^{-1} and reaches equilibrium at an absorbance of 0.012. Therefore, the critical concentration of $Ru(bpy)_3^{2+}$ for the color change of 2 pM of the 97 nm Au nanoparticles is 1.17 μM. TEM images of the 97 nm Au nanoparticles (2 pM) in the absence and presence of $Ru(bpy)_3^{2+}$ (0, 1.30 μM) in Figure 4C, D show that the individual Au nanoparticles are well isolated in the absence of $Ru(bpy)_3^{2+}$, and only a very few nanoparticles interact with each other after their incubation with 1.30 μM $Ru(bpy)_3^{2+}$ for 2 h. The result suggests that the coagulation of Au nanoparticles is not the sole factor that causes the color change of the 97 nm Au nanoparticles. The control experiment is performed by incubating 2 pM of the 97 nm Au nanoparticles with 5.2 μM NaCl and $MgCl_2$ (4-fold higher than the critical concentration of $Ru(bpy)_3^{2+}$), showing that the peak absorbance of the 97 nm Au nanoparticle solution remains constant (Figure 4B) and the color of the Au nanoparticle solution is unchanged. TEM images of the 97 nm Au nanoparticle solution incubated with 5.2 μM NaCl or $MgCl_2$ for 2 h are similar to those observed in the absence of $Ru(bpy)_3^{2+}$, showing the well-isolated individual Au nanoparticles (Figure 4C) and demonstrating that the salt effect seems not to play a major role in changing the color of the 97 nm Au nanoparticle solution.

Taken together, the results indicate that the color-change kinetics of the Au nanoparticles induced by $Ru(bpy)_3^{2+}$ is highly dependent upon the size of nanoparticles and $Ru(bpy)_3^{2+}$ concentration. In Table 1, we summarize the critical concentrations of $Ru(bpy)_3^{2+}$ needed for color change of the Au nanoparticles and its dependence upon the nanoparticle sizes, the surface Au atoms of the individual nanoparticle, and the total surface Au atoms of all nanoparticles in the solution. It appears that the higher molar ratio of $Ru(bpy)_3^{2+}$ to Au nanoparticles is required to change the color of the larger Au nanoparticles. For instance, the molar ratio of $Ru(bpy)_3^{2+}$ to the 19, 48, and 97 nm Au nanoparticles of 3.0×10^2, $1.4 \times$

TABLE 1: Minimum Concentrations of $Ru(bpy)_3^{2+}$ Needed for the Color Change of Au Nanoparticle Solutions

diameter of Au nanopaticle (nm)	6.5 ± 1.5	18.6 ± 3.5	48.1 ± 5.8	96.7 ± 15.4
C, Au nanoparticle (pM)	2.13×10^3	3.60×10^2	6	2
surface Au atoms per nanoparticle[a]	2×10^3	1×10^4	9×10^4	4×10^5
total surface Au atoms of all nanoparticles in the solution[b]	7×10^{15}	1×10^{16}	1×10^{15}	2×10^{15}
C, $Ru(bpy)_3^{2+}$ (nM)[c]		107	83	1170
molar ratio, $Ru(bpy)_3^{2+}$/Au nanoparticle = number of $Ru(bpy)_3^{2+}$ molecules per Au nanoparticle		3.0×10^2	1.4×10^4	6.0×10^5
molar ratio, $Ru(bpy)_3^{2+}$/surface Au atoms of a nanoparticle		2×10^{10}	2×10^9	7×10^9
molar ratio, $Ru(bpy)_3^{2+}$/total surface Au atoms		0.02	0.2	2
maximum adsorbed $Ru(bpy)_3^{2+}$ per nanoparticle (molecules)[d]	79	8×10^2	4×10^3	2×10^4

[a] The surface Au atoms of an individual Au nanoparticle are calculated by dividing the surface area of an individual Au nanoparticle (πD^2) with the area of an individual Au atom (diameter of Au atom (d_{Au}) = 0.288 nm; area = d_{Au}^2) using a close-pack model. D = 6.5, 19, 48, and 97 nm. [b] The total number of surface Au atoms is calculated by dividing the surface area of all Au nanoparticles (πD^2NCV) in the solution with the area of an individual Au atom (diameter of Au atom (d_{Au}) = 0.288 nm; area = d_{Au}^2) using a close-pack model, where *D*, *N*, *C*, and *V* refer to diameter of Au nanoparticles (6.5, 19, 48, and 97 nm), Avogadro's constant (6.02×10^{23}), concentration of the Au nanoparticles, and volume of Au nanoparticle solution, respectively. [c] The minimum concentration of $Ru(bpy)_3^{2+}$ needed to change the color of the Au nanoparticle solutions is determined experimentally as shown in Figures 1−4. [d] The maximum number of a monolayer of $Ru(bpy)_3^{2+}$ molecules adsorbed on the surface of an individual Au nanoparticle (D = 6.5, 19, 48, and 97 nm) is theoretically calculated by dividing the surface area of an individual Au nanoparticle (πD^2) with the area of an individual $Ru(bpy)_3^{2+}$ molecule (diameter of $Ru(bpy)_3^{2+}$ molecules (d) = 1.3 nm; area = d^2) using a close-pack model.

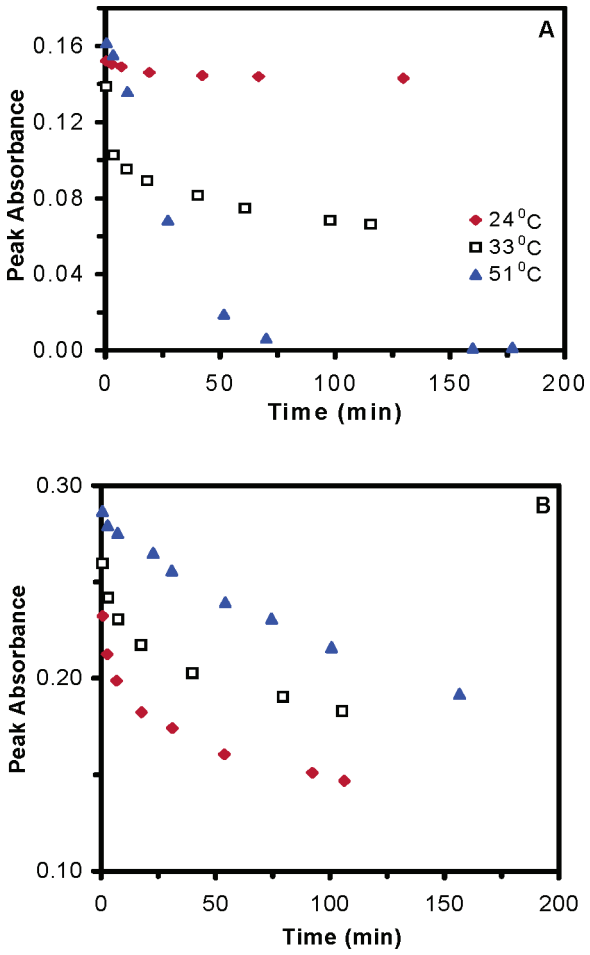

Figure 5. Color-change kinetics of the Au nanoparticles shows the temperature dependence and size dependence. Representative plots of baseline-subtracted peak absorbance at 524 nm versus incubation time are constructed from the absorbance spectra of the solution: (A) 0.360 nM of the 19 nm Au nanoparticle solution containing 107 nM $Ru(bpy)_3^{2+}$ at (◆) 24.0 °C, (□) 33.0 °C, (▲) 51.0 °C; (B) 6 pM of the 48 nm Au nanoparticle solution containing 76 nM $Ru(bpy)_3^{2+}$ at (◆) 24.0 °C, (□) 33.0 °C, (▲) 51.0 °C.

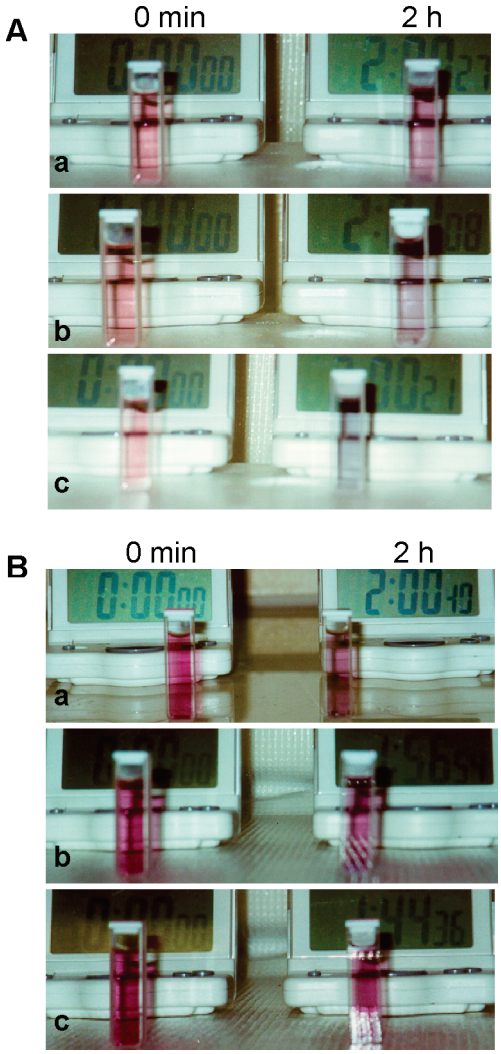

Figure 6. Representative color photos of the Au nanoparticle solutions are acquired from experiments in Figure 5, showing temperature dependence. (A) The 19 nm Au nanoparticles (0.360 nM) before (0 min) (left) and after incubation with 107 nM $Ru(bpy)_3^{2+}$ for 2 h (right) at (a) 24.0 °C, (b) 33.0 °C, (c) 51.0 °C. (B) The 48 nm Au nanoparticles (6 pM) before (0 min) (left) and after incubation with 76 nM $Ru(bpy)_3^{2+}$ for 2 h (right) at (a) 24.0 °C, (b) 33.0 °C, (c) 51.0 °C.

10^4, and 6.0×10^5 is needed to change the color of the Au nanoparticles, respectively. By comparing the molar ratio of $Ru(bpy)_3^{2+}$ to the Au nanoparticles (number of $Ru(bpy)_3^{2+}$ molecules per Au nanoparticle) with the theoretically calculated monolayer of $Ru(bpy)_3^{2+}$ molecules adsorbed on the surface of the individual nanoparticle, we find that more than a monolayer of $Ru(bpy)_3^{2+}$ is required to change the color of the 97 nm Au nanoparticles, whereas less than a monolayer of $Ru(bpy)_3^{2+}$ is needed to change the color of the 19 and 48 nm Au nanoparticles.

The molar ratio of $Ru(bpy)_3^{2+}$ to the surface Au atoms of the individual 48 nm Au nanoparticle (2×10^9) is 10-fold lower than that of the individual 19 nm Au nanoparticle (2×10^{10}). Note that the surface Au atoms of the individual 48 nm Au nanoparticle (9×10^4) are about 10-fold higher than that of the individual 19 nm Au nanoparticle (1×10^4). The molar ratio of $Ru(bpy)_3^{2+}$ to the total surface Au atoms of all 48 nm Au nanoparticles in the solution (0.2) is 10-fold higher than that of all 19 nm Au nanoparticles (0.02). Note that the total surface Au atoms of the 48 nm Au nanoparticles (1.1×10^{15}) are 10-fold lower than that of the 19 nm Au nanoparticles (1.0×10^{16}).

These results show that the critical concentration of $Ru(bpy)_3^{2+}$ needed to change the color of the 19, 48, and 97 nm Au nanoparticles is highly associated with the number of surface Au atoms of the individual nanoparticle and the total number of Au atoms of all nanoparticles in the solution, suggesting that the color-change mechanism of the Au nanoparticles induced by $Ru(bpy)_3^{2+}$ may indeed involve the adsorption of $Ru(bpy)_3^{2+}$ on the surface of Au nanoparticles.

Temperature Dependence. The measurements in Figures 1−4 (Table 1) are carried out at room temperature (~24 °C). Interestingly, we notice that the critical concentration of $Ru(bpy)_3^{2+}$ for the color change of Au nanoparticles is highly sensitive to the temperature and varies slightly over the fluctuations of the room temperature. To investigate whether the temperature dependence of the color change of Au nanoparticles is associated with the size of nanoparticles, two representative sizes of Au nanoparticles, 19 and 48 nm, are selected to study the color-change kinetics of the Au nanoparticles at 24.0, 33.0, and 51.0 °C. The Au nanoparticle solution is incubated with the critical concentration of $Ru(bpy)_3^{2+}$ at a constant temperature (24.0, 33.0, or 51.0 °C), and the spectra of the Au nanoparticle solution are recorded over 2 h. Plots of the peak absorbance of the Au nanoparticle solutions containing the critical concentration of $Ru(bpy)_3^{2+}$ versus time at 24.0, 33.0, and 51.0 °C (Figure 5) show that the rate of color change of

Au nanoparticles induced by $Ru(bpy)_3^{2+}$ highly depends on the temperature.

In the presence of the critical concentration of $Ru(bpy)_3^{2+}$, the rate of decreased absorbance (color change) of Au nanoparticles is strikingly sensitive to the temperature and the size of nanoparticles. In Figure 5A, no significant color change is observed over 2 h as 0.36 nM of the 19 nm Au nanoparticle solution is incubated with 0.107 μM $Ru(bpy)_3^{2+}$ at 24.0 °C for 2 h. As the temperature of the solution increases to 33.0 °C, the pink color of the Au nanoparticle solution vanishes and turns to light blue within 20 min of incubation time (Figure 6A). Once the color changes from pink to blue, the reaction becomes an irreversible process. A similar phenomena is observed at 51.0 °C with 2-fold and 8-fold higher reaction rate than at 33.0 and 24.0 °C, respectively. A blank control experiment is performed by incubation of the Au nanoparticles with 524 nM NaCl or $MgCl_2$ (4-fold higher than the critical concentration of $Ru(bpy)_3^{2+}$) for 2 h, indicating no color change at 24.0−51.0 °C. UV−vis absorbance spectra of the $Ru(bpy)_3^{2+}$ solution in the absence of Au nanoparticles at 24.0−51.0 °C have also been measured, indicating no change of $Ru(bpy)_3^{2+}$ absorbance and further confirming the chemical stability of $Ru(bpy)_3^{2+}$.

In contrast to the results of the 19 nm Au nanoparticles, the surface plasmon absorbance of the 48 nm Au nanoparticle solution in the presence of the critical concentration (76 nM) of $Ru(bpy)_3^{2+}$ decreases with time more rapidly at the lower temperature (Figure 5B) (3-fold higher at 24.0 °C than at 51.0 °C). The surface plasmon absorbance (color) of 6 pM of the 48 nm Au nanoparticles changes with time at 24.0 °C with the addition of 76 nM $Ru(bpy)_3^{2+}$. Surprisingly, the plasmon absorbance of the 48 nm Au nanoparticles solution decreases much more slowly at the higher temperature (33.0 and 51.0 °C) and reaches equilibrium at a concentration that is 2-fold higher at 51 °C than that at 24 °C. This result suggests that the reaction rate decreases as the temperature increases. The Au nanoparticle solution containing 76 nM $Ru(bpy)_3^{2+}$ remains its original pink color at 33.0 and 51.0 °C for 2 h (Figure 6B). A blank control experiment is performed by incubating the Au nanoparticles with 5.2 μM NaCl or $MgCl_2$ concentration (4-fold higher than the critical concentration of $Ru(bpy)_3^{2+}$) for 2 h, indicating no color change at 24.0−51.0 °C.

The refractive index of water changes with temperature, which may cause the blue shift and lower plasmon absorption of Au nanoparticles and may obscure our observation of true temperature dependence of the surface plasmon absorption of Au nanoparticles. To rule out such a possibility, we perform the blank control experiment in the absence of $Ru(bpy)_3^{2+}$, demonstrating that the plasmon absorption of the 19 and 48 nm Au nanoparticles remains unchanged at 24.0−51.0 °C. The other blank control experiment is performed by incubating the Au nanoparticles with a concentration of NaCl or $MgCl_2$ that is 4−10-fold higher than the critical concentration of $Ru(bpy)_3^{2+}$, indicating no color change of the Au nanoparticles at 24.0−51.0 °C. These results confirm that the observed temperature dependence of the color change of Au nanoparticles shown in Figures 5 and 6 is not attributable to the change of the refractive index of water.

Taken together, the results in Figure 5 show that the color-change rate of Au nanoparticle solutions induced by $Ru(bpy)_3^{2+}$ is highly dependent upon the temperature and nanoparticle size. On the basis of kinetic theory, as temperature increases, the rate of $Ru(bpy)_3^{2+}$ adsorbed on the Au nanoparticle surface decreases whereas the rate of $Ru(bpy)_3^{2+}$ neutralizing the surface charges of Au nanoparticles increases. The former decreases the color-change rate of the Au nanoparticle solution. In contrast, the latter accelerates the color-change kinetics. For the smaller Au nanoparticles (19 nm in diameter), as temperature increases, the rate of surface charges of Au nanoparticles neutralized by $Ru(bpy)_3^{2+}$ increases much more rapidly than the decreased rate of $Ru(bpy)_3^{2+}$ adsorbed on the Au nanoparticle surface, due to individual smaller nanoparticles (19 nm) having smaller surface area and less negative charges than individual larger nanoparticles (48 nm). Thus, the salt effect (neutralization of surface charges of nanoparticles) for the smaller nanoparticles is more sensitive to the temperature change and plays a more pronounced role in changing the surface plasmon absorption of Au nanoparticles. Consequently, the color-change rate of the 19 nm Au nanoparticles increases as the temperature increases. In contrast, for the larger nanoparticles (48 nm), as the temperature increases, the rate of $Ru(bpy)_3^{2+}$ adsorbed on the surface of Au nanoparticles decreases more significantly than the increased rate of neutralization of surface charges of nanoparticles by $Ru(bpy)_3^{2+}$ (salt effect), owing to the larger surface area and more surface negative charges of individual 48 nm Au nanoparticles. Thereby, the adsorption effect is a dominant mechanism and plays a leading role in changing the color of the 48 nm Au nanoparticles. As a result, the color-change rate of the 48 nm Au nanoparticles decreases as temperature increases.

These plausible explanations may help to understand why the results from this study appear different from the reported findings[3,4,21,41] and proposed models,[18,52,53] which describe the small temperature dependence of surface plasmon absorbance (color) of colloidal Au nanoparticles and the smaller temperature dependence of the larger Au nanoparticles. According to the chemical interface-damping model,[52,53] the Fermi distribution of electrons varies with temperature. Higher temperatures lead to a larger population of the higher electronic states, which can undergo a charge transfer into the acceptor level.[16,51−53] This model and previous studies show that the temperature dependence of surface plasmon absorption of Au nanoparticles[21,22,41] is very small and nearly negligible.

In this study, in the presence of the critical concentration of $Ru(bpy)_3^{2+}$, we find that the surface plasmon absorption of Au nanoparticles shows astonishingly high dependence upon temperature, indicating that the plasmon absorbance of the Au nanoparticles decreases more rapidly at higher temperatures for the 19 nm Au nanoparticles (8-fold higher at 51.0 °C than at 24.0 °C) (Figure 5A), whereas the absorbance of the Au nanoparticles decreases more rapidly at lower temperatures for the 48 nm Au nanoparticles (3-fold higher at 24.0 °C than at 51.0 °C). The strikingly high temperature dependence suggests that other mechanisms, such as adsorption and de-adsorption of $Ru(bpy)_3^{2+}$ on the Au nanoparticle surface, chemical reaction of $Ru(bpy)_3^{2+}$ with the surface Au atoms, or charge transfer between ligand, tris(2,2′-bipyridine), with surface plasmon, may be involved in changing the color of Au nanoparticles. This study provides new insights into the size dependence and temperature dependence of surface plasmon absorption of Au nanoparticles in the presence of surface adsorbates, demonstrating a new approach for the color change of Au nanoparticle solutions using temperature and surface adsorbates.

Even though the absorbance of $Ru(bpy)_3^{2+}$ in Figure 4A indicates that $Ru(bpy)_3^{2+}$ remains constant over the incubation time, such measurement of $Ru(bpy)_3^{2+}$ is limited by the detection limit of UV−vis absorbance spectroscopy. Therefore, we have not yet completely eliminated the possibility of chemical reaction between $Ru(bpy)_3^{2+}$ and the Au nanoparticles.

We have detected single $Ru(bpy)_3^{2+}$ molecules in solution using single molecule microscopy and spectroscopy.[49,55] Efforts are in progress to further investigate the effect of $Ru(bpy)_3^{2+}$ upon the color-change mechanism of Au nanoparticles at the molecular level.

Conclusions

In conclusion, we have studied the color-change kinetics of the colloidal Au nanoparticles (6.5, 19, 48, 97 nm) induced by a variety of concentrations of $Ru(bpy)_3^{2+}$ at 24.0, 33.0, and 51.0 °C. The new findings are summarized as follows. (i) The minimum (critical) concentration of $Ru(bpy)_3^{2+}$ needed to change the color of the Au nanoparticles is highly dependent upon temperature, the size of nanoparticles, the surface Au atoms of the individual nanoparticle, and the total surface Au atoms of all nanoparticles in the solution. (ii) The surface plasmon absorption (color) of Au nanoparticle solutions in the presence of the critical concentration of $Ru(bpy)_3^{2+}$ is highly sensitive to temperature and nanoparticle size, suggesting that the surface plasmon absorption of Au nanoparticle solutions can be altered by temperature and the surface adsorbates, $Ru(bpy)_3^{2+}$. (iii) The color-change rate of Au nanoparticles is highly sensitive to the $Ru(bpy)_3^{2+}$ concentration. For example, the rate of the 19 nm Au nanoparticles (0.36 nM) changes 3-fold in response to a variation of 7 pmol of $Ru(bpy)_3^{2+}$. Taken together, these findings suggest the possibility of ultrasensitive analysis of surface adsorbates using the colorimetry of Au nanopartices and the design of optical properties of Au nanoparticles by modification of Au nanoparticle surfaces with specific adsorbates. These findings also open up new opportunities for the study of photochemistry of $Ru(bpy)_3^{2+}$ on Au nanoparticle surfaces.

Acknowledgment. The support of this work in part by NIH (RR15057-01) and Old Dominion University, Dominion Scholar Fellowship (S.H. and R.B.J.), University Summer Graduate Research Assistantship (W.B.), and Old Dominion Honor College Undergraduate Research Fellowship (K.S.) is gratefully acknowledged.

References and Notes

(1) Mulvaney, P. *Langmuir* **1996**, *12* (3), 788.
(2) Kharitonov, A. B.; Shipway, A. N.; Willner, I. *Anal. Chem*. **1999**, *71*, 5441.
(3) McConnell, W. P.; Novak, J. P.; Brousseau, L. C., III; Fuierer, R. R.; Tenent, R. C.; Feldheim, D. L. *J. Phys. Chem.* **2000**, *104*, 8925, and references therein.
(4) Whyman, R. *Gold Bull.* **1996**, *29* (1), 11.
(5) Mie, G. *Ann. Phys*. **1908**, *25*, 377.
(6) Bohren, C. F.; Huffman, D. R. *Absorption and Scattering of Light by Small Particles*; Wiley: New York, 1983; pp 287−380, and references therein.
(7) Kreibig, U.; Vollmer, M. *Optical Properties of Metal Clusters*; Springer: Berlin, 1995; pp 14−123, and references therein.
(8) Haes, A. J.; Van Duyne, R. P. *J. Am. Chem. Soc.* **2002**, *124*, 10596, and references therein.
(9) Handley, D. A. The development and application of colloidal gold as a microscopic probe. In *Colloid Gold: Principles, Methods and Applications*; Hayat, M. A., Ed.; Academic Press: New York, 1989; Vol. 1, pp 1−8.
(10) Grabar, K.; Freeman, R.; Hommer, M.; Natan, M. *Anal. Chem*. **1995**, *67*, 735, and references therein.
(11) Wada, Y.; Hamasaki, T.; Satir, P. *Mol. Biol. Cell* **2000**, *11* (1), 161, and references therein.
(12) Mirkin, C. A.; Letsinger, R. L.; Mucic, R. C.; Storhoff, J. J. *Nature* **1996**, *382*, 607.
(13) Xu, X.-H. N.; Chen, J.; Jeffers, R. B.; Kyriacou, S. *Nano Lett.* **2002**, *2*, 175.
(14) Sandhu, K.; Simard, J.; McIntosh, C.; Smith, S.; Rotello, V. *Bioconj. Chem*. **2002**, *13*, 3−6.
(15) Xu, X.-H. N.; Patel, R. Nanoparticles for live cell dynamics. In *Encyclopedia of Nanoscience and Nanotechnology*; Nalwa, H. S., Ed.; American Scientific Publishers: CA, 2004; Vol. 7, pp 181−192.
(16) Kyriacou, S. V.; Brownlow, W.; Xu, X.-H. N. *Biochemistry* **2004**, *43* (2), 140−147; Xu, X.-H. N.; Brownlow, W.; Kyriacou, S. V.; Wan, Q.; Viola, J. J. *Biochemistry* **2004**, *43* (32), 10400−10413.
(17) Xu, X.-H. N.; Patel, R. Imaging and assembly of nanoparticles in biological systems. In *Handbook of Nanostructured Biomaterials and Their Applications in Nanobiotechnology*; Nalwa, H. S., Ed.; American Scientific Publishers: CA, 2004; Vol. 1 (in press).
(18) Teranishi, T.; Haga, M.; Shiozawa, Y.; Miyake, M. *J. Am. Chem. Soc*. **2000**, *122* (17), 4237.
(19) Link, S.; El-Sayed, M. A. *J. Phys. Chem. B* **1999**, *103* (21), 8410, and references therein.
(20) Kreibig, U.; Genzel, U. *Surf. Sci.* **1985**, *156*, 678.
(21) Kimura, K. *Surf. Rev. Lett.* **1996**, *3*, 1219, and references therein.
(22) Shipway, A. N.; Lahav, M.; Gabai, R.; Willner, I. *Langmuir* **2000**, *16*, 8789, and reference therein.
(23) Brown, K. R.; Walter, D. G.; Natan, M. J. *Chem. Mater*. **2000**, *12*, 306, and references therein.
(24) Ahmadi, T. S.; Logunov, S. L.; El-Sayed, M. A. *ACS Symp. Ser. Nanostruct. Mater*. **1997**, *679*, 125−140, and references therein.
(25) Hodak, J. H.; Henglein, A.; Hartland, G. V. *Pure. Appl. Chem.* **2000**, *72*, 189, and references therein.
(26) Zamborini, F. P.; Hicks, J. F.; Murray, R. W. *J. Am. Chem. Soc.* **2000**, *122*, 4514.
(27) Templeton, A. C.; Hostetler, M. J.; Kraft, C. T.; Murray, R. W. *J. Am. Chem. Soc.* **1998**, *120*, 1906.
(28) Petta, J. R.; Salinas, D. G.; Ralph, D. C. *Appl. Phys. Lett.* **2000**, *77*, 4419.
(29) Eck, D.; Helm, C. A. *Langmuir* **2001**, *17*, 957.
(30) Sato, S.; Toda, K.; Oniki, S. *J. Colloid. Interface Sci.* **1999**, *218*, 504.
(31) Anderson, M. L.; Morris, C. A.; Stroud, R. M.; Merzbacher, C. I.; Rolison, D. R. *Langmuir* **1999**, *15*, 674.
(32) Musick, M. D.; Keating, C. D.; Keefe, M. H.; Natan, M. J. *Chem. Mater*. **1997**, *9*, 1499.
(33) Brown, L. O.; Hutchison, J. E. *J. Am. Chem. Soc.* **1999**, *121*, 882.
(34) Lyon, L. A.; Pena, D. J.; Natan, M. J. *J. Phys. Chem. B* **1999**, *103*, 5826.
(35) Park, S.-H.; Im, J.-H.; Im, J.-W.; Chun, B.-H., Kim, J.-H. *Microchem. J*. **1999**, *63*, 71.
(36) Davidović, D.; Tinkham, M. *Phys. Rev. Lett.* **1999**, *83*, 1644.
(37) Ghaddar, T. H.; Wishart, J. F.; Kirby, J. P.; Whitesell, J. K.; Fox, M. A. *J. Am. Chem. Soc*. **2001**, *123* (51), 12832.
(38) Han, M. Y.; Quek, C. H. *Langmuir* **2000**, *16*, 362.
(39) Demers, L. M.; Mirkin, C. A.; Mucic, R. C.; Reynolds, R. A.; Letsinger, R. L.; Elghanian, R.; Viswanadham, G. *Anal. Chem.* **2000**, *72*, 5535.
(40) Link, S.; Burda, C.; Wang, Z. L.; El-Sayed, M. A. *J. Chem. Phys.* **1999**, *111*, 1255.
(41) Link, S.; El-Sayed, M. A. *J. Phys. Chem. B* **1999**, *103*, 4212.
(42) Maye, M. M.; Chun, S. C.; Han, L.; Rabinovich, D.; Zhong, C.-J. *J. Am. Chem. Soc*. **2002**, *124*, 4958.
(43) Shipway, A. N.; Lahav, M.; Blonder, R.; Willner, I. *Chem. Mater*. **1999**, *11*, 13.
(44) Lahav, M.; Heleg-Shabtai, V.; Wasserman, J.; Katz, E.; Willner, I.; Dürr, H.; Hu, Y.-Z.; Bossmann, S. H. *J. Am. Chem. Soc.* **2000**, *122*, 11480.
(45) Roundhill, D. M. Photochemistry and Photophysics of Metal Complexes. In *Modern Inorganic Chemistry*; Fackler, J. P., Ed.; Plenum: New York, 1994; pp 165−169, and references therein.
(46) Blackburn, G.; Shah, H. P.; Kenten, J.; Leland, J.; Kamin, R.; Link, J.; Peterman, J.; Powell, M.; Shah, A.; Talley, D.; Tyagi, S.; Wilkins, E.; Wu, T.; Massey, R. *Clin. Chem.* **1991**, *37/9*, 1534.
(47) Bard, A. J.; Debad, J.; Leland, J.; Signal, G.; Wilbur, J.; Wohlstadter, J. Analytical Applications of Electrogenerated Chemiluminescence. In *Encyclopedia of Analytical Chemistry: Instrumentation and Applications*; Meyers, R. A., Ed.; Wiley: New York, 2000; Vol. 11, pp 9842−9848, and references therein.
(48) Xu, X.-H.; Yang, H.; Mallouk, T. E.; Bard, A. J. *J. Am. Chem. Soc*. **1994**, *116*, 8386.
(49) Xu, X.-H. N.; Jeffers, R.; Gao, J.; Logan, B. *Analyst* **2001**, *126*, 1285.
(50) Xu, X.-H.; Bard, A. J. *Langmuir* **1994**, *10*, 2409.
(51) Huang, T.; Murray, R. W. *Langmuir* **2002**, *18*, 7077.
(52) Hövel, H.; Fritz, S.; Hilger, A.; Kreibig, U. *Phys. Rev.* **1993**, *48*, 18178.
(53) Perner, M.; Bost, P.; Lemmer, U.; Plessen, G.; Feldmann, J. *Phys. Rev. Lett.* **1997**, *78*, 2192.
(54) Handley, D. A. Methods for synthesis of colloidal gold. In *Colloid Gold: Principles, Methods and Applications*; Hayat, M. A., Ed.; Academic Press: New York, 1989; Vol. 1, pp 15−27.
(55) Xu, X.-H.; Gao, J.; Jeffers, R.; Logan, B. Molecular Analysis of Biomarkers for the Earlier Cancer Detection. In *Scanning and Force Microscopies for Biomedical Applications II*; Nie, S., Tamiya, E., Yeung, E. S., Eds.; Proceedings of the SPIE, 2000; Vol. 3922, p 15.